J Solid State Electrochem (2012) 16:3725–3738
DOI 10.1007/s10008-012-1803-7

ORIGINAL PAPER

One-step electrosynthesis of poly(3,4-ethylenedioxy-thiophene)–ethylsulfate matrix for fabricating vitamin C electrochemical biosensor and its determination in commercial juices

Yangping Wen · Xuemin Duan · Jingkun Xu · Ruirui Yue · Dong Li · Ming Liu · Limin Lu · Haohua He

Received: 18 August 2011 / Revised: 16 April 2012 / Accepted: 20 June 2012 / Published online: 12 July 2012

Abstract A stable and specific electrochemical biosensor based on a poly(3,4-ethylenedioxythiophene)–ethyl sulfate (PEDOT–$EtSO_4$) matrix with high conductivity and stability was easily fabricated. 1-Ethyl-3-methylimidazolium ethyl sulfate ([Emim][$EtSO_4$]), a halogen-free and relatively hydrolysis-stable hydrophilic ionic liquid, was selected as the supporting electrolyte for the one-step electrosynthesis of the PEDOT–$EtSO_4$ matrix under the optimum conditions. The PEDOT–$EtSO_4$ matrix electrosynthesized in the [Emim][$EtSO_4$] aqueous solution displayed high conductivity and stability. Inspired by preceding studies, the electrochemical biosensor based on the resulting PEDOT–$EtSO_4$ matrix was facilely developed to determine the vitamin C (VC) level in commercial juices. Ascorbate oxidase (AO) was dip-coated on the surface of the as-prepared matrix, then Nafion was covered on the surface of AO layers for preventing the leakage of enzyme molecules. The fabricated biosensor displayed an excellent bioelectrocatalytic activity to the oxidation of VC. Under optimal conditions, the fabricated amperometric biosensor showed rapid response (less than 2 s) to VC at a low potential of 0.2 V over a wide range of concentrations from 8.0×10^{-7} to 1×10^{-3} M with a high sensitivity of 104.8 mA M^{-1} cm^{-2}, and the limit of detection and the limit of quantification of presented method was 0.147 μM and 0.487 μM, respectively. Moreover, the bioaffinity, specificity, stability, and reproducibility of the biosensor were also evaluated. Finally, the biosensor was employed to determine the content of VC in commercial juice samples by amperometric and voltammetric methods. The satisfactory results indicated that the as-prepared conducting PEDOT–$EtSO_4$ films as immobilization matrix of biologically active species could be a promising candidate for the design and application of biosensors.

Keywords Biosensors · Poly(3,4-ethylenedioxythiophene) · Ionic liquids · Ascorbate oxidase · Vitamin C

Electronic supplementary material The online version of this article (doi:10.1007/s10008-012-1803-7) contains supplementary material, which is available to authorized users.

Y. Wen · D. Li · M. Liu · L. Lu · H. He (✉)
Key Laboratory of Crop Physiology, Ecology and Genetic Breeding, Ministry of Education, and Key Laboratory of Physiology, Ecology and Cultivation of Double Cropping Rice, Ministry of Agriculture, Jiangxi Agricultural University, Nanchang 330045, People's Republic of China
e-mail: hhhua64@163.com

Y. Wen · J. Xu (✉) · R. Yue · D. Li · M. Liu
Jiangxi Key Laboratory of Organic Chemistry, Jiangxi Science and Technology Normal University, Nanchang 330013, People's Republic of China
e-mail: xujingkun@tsinghua.org.cn

X. Duan
School of Pharmacy, Jiangxi Science & Technology Normal University, Nanchang 330013, People's Republic of China

Introduction

The electrochemistry of inherently conducting polymers (ICPs) in ionic liquids (ILs) has attracted considerable attention in recent years [1–3]. Moreover, the utility of ICPs in ILs is very promising for actuators, batteries, supercapacitors, light-emitting electrochemical cells, electrochromic windows and displays, photovoltaic cells, sensors, and biosensors [3–6].

Anions of the most common ILs are mainly halogen anions such as hexafluorophosphate anion and tetrafluoroborate anion [7]. These ions are known to be decomposed in water; as a result, toxic and corrosive species such as hydrofluoric and phosphoric acids are formed [7, 8], which has an adverse effect on the bioactivity of organism, tissue, cell, and biologically active macromolecules. Interestingly, ILs with alkyl

sulfate anions are halide-free and relatively hydrolysis-stable compounds, which would be a promising alternative to industrial application. These ions can avoid the liberation of toxic and corrosive materials into the environment Thus, ILs with alkyl sulfate anions are very beneficial to improve the performance of biosensors, especially biosensors intimately associated with biologically active species.

1-Ethyl-3-methylimidazolium ethyl sulfate ([Emim][$EtSO_4$], Scheme 1) is one of halogen-free and relatively hydrolysis-stable ILs with alkyl sulfate anions. In addition to physicochemical properties of the most common ILs, [Emim][$EtSO_4$] also possesses a number of desirable features such as simple preparation, low cost, non-toxicity, hydrophilicity, and stability in air [9]. [Emim][$EtSO_4$] has been attracting increasing attention due to amazing physicochemical properties [10–16] since this ionic liquid [9] was firstly synthesized. Meanwhile, [Emim][$EtSO_4$] has also been the focus of many scientific investigation for widespread application such as extraction [17], separation [18, 19], synthesis [20, 21], catalysis [22], solubility [23], and the design of highly sensitive and selective biosensors [24–29]. In conclusion, [Emim][$EtSO_4$], the availability, application, and combination of a wide range of ICPs with new biosensing techniques, could cause a remarkable innovation in the design and construction of biosensing devices, especially the electrochemical ones. Recently, Bernardes et al. [30] reported four distinct structural regimes of [Emim][$EtSO_4$] aqueous solution in the full concentration range (isolated water molecules, chain-like water aggregates, bicontinuous system, and isolated ions or small ion clusters). Moreover, [Emim][$EtSO_4$] aqueous solution is also a cost-efficient and "green" solvent system for electrochemistry. Therefore, the preparation of high-performance and non-toxicity ICPs in [Emim][$EtSO_4$] aqueous solution system is significant in the immobilization of biologically active species.

Poly(3,4-ethylenedioxythiophene) (PEDOT), one of the most stable and promising ICPs currently available, has been widely applied in the development and application of electrochemical biosensors and used as immobilization materials of biologically active species. Recently, the electrochemical synthesis and behaviors of PEDOT films in ILs system with various pure ILs have been reported [31–37], and their properties and application in sensing and biosensing devices have also been studied. These biosensors fabricated in ILs exhibited excellent performance and good anti-interference to impurities [38, 39], which is very beneficial to the design and application of biosensors.

Biosensor technology as a novel method for the determination of VC can overcome many disadvantages of traditional methods, including tedious and time-consuming multi-step procedures, interference resulting from colored substances or impurities present in real samples, and the high cost of equipment, reagent, and operator training [40–42]. Enzymatic method is more sensitive, accurate, specific, and efficient than traditional methods. Unfortunately, the use of expensive ascorbate oxidase (AO; EC 1.10.3.3, Scheme 1) in routine measurement is uneconomical. The AO-based biosensor technology for the determination of vitamin C (VC) is an economical, practical, specific, accurate, fast, efficient, and sensitive method. Hence, a variety of AO-based biosensors for the direct or indirect determination of VC content were developed by different materials and methods (Table S3). Moreover, electrochemical methods have also been employed for the fabrication of efficient biosensors either directly or in combination with other analytical methods [43–45].

Water is still an excellent, non-toxic, and inexpensive solvent system compared with other solvent system in electrochemistry of ICPs. Hence, an ionic liquid–water mixture system is an excellent, non-toxic, and cost-effective system for electrochemistry of ICPs by combing advantages of the two. In our previous work, the electrosynthesis of PEDOT films in ILs/surfactant/H_2O system indicated that IL-in-water (IL/W) was the optimal system for the electropolymerization of EDOT in comparison with water-in-IL (W/IL) and bicontinuous, while the electropolymerization of EDOT did not happen in W/IL [46]. In addition, AO-based electrochemical biosensors based on PEDOT–carbon nanotubes for the detection of VC have also been studied [47, 48]. To the best of our knowledge, so far, there is no report on the fabrication of the biosensor based on the PEDOT–$EtSO_4$ matrix.

In the present work, the electrochemical synthesis and behavior of PEDOT–$EtSO_4$ films were investigated in aqueous solution containing various concentrations of [Emim][$EtSO_4$]. Then a novel electrochemical biosensor based on the entrap immobilization of AO on the surface of PEDOT–$EtSO_4$ modified glassy carbon disk electrode (GCE) for amperometric and voltammetric detection of VC was simply fabricated. Finally, the performance of the as-fabricated PEDOT–$EtSO_4$/AO/Nafion biosensor was evaluated, and the VC in commercial juices was also electrochemically determined using the obtained biosensor at the same time.

Experimental section

Chemicals

AO (from cucumber *Cucurbita* sp), EDOT, and poly(sodium 4-styrenesulfonate) (NaPSS, molar mass=70,000) were purchased from Aldrich. [Emim][$EtSO_4$] was obtained from Tokyo Chemical Industry Co., Ltd. Five percent Nafion solution was obtained from DuPont Co., Ltd. Disodium hydrogen phosphate dodecahydrate ($Na_2HPO_4{\cdot}12H_2O$), sodium dihydrogen phosphate dihydrate ($NaH_2PO_4{\cdot}2H_2O$), lithium perchlorate trihydrate ($LiClO_4{\cdot}3H_2O$), and potassium chloride (KCl) were purchased from Sinopharm

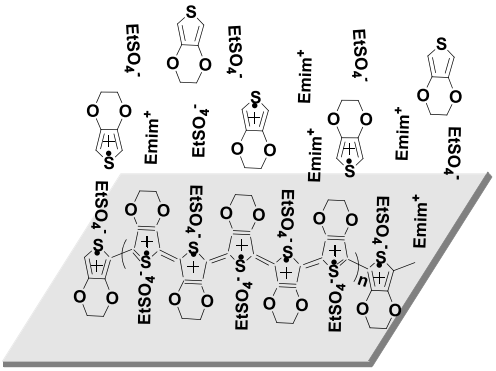

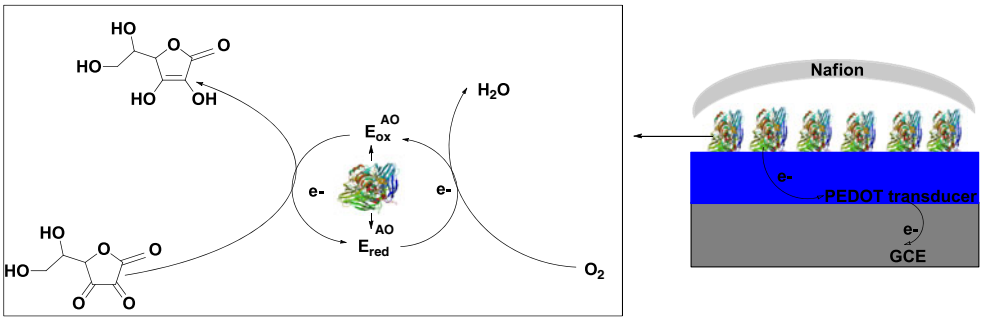

Scheme 1 Electrochemical preparation procedures and mechanism of PEDOT–$EtSO_4$ matrix in [Emim][$EtSO_4$] aqueous solution containing EDOT, and the working mechanism of the fabricated biosensor for the detection of VC

Chemical Reagent Co., Ltd. Fifty millimolar of phosphate-buffered solution (PBS, pH=6.5) was prepared from 50 mM $NaH_2PO_4{\cdot}2H_2O$ aqueous solution and 50 mM $Na_2HPO_4{\cdot}12H_2O$ aqueous solution. VC was purchased from Bio Basic Inc. All reagents were analytical grade and used as received without further purification. All solutions were prepared using deionized distilled water.

Electrochemical measurements

All electrochemical experiments were performed in a three-electrode cell. A GCE with a diameter of 3 mm was used as working electrode, and a platinum wire with a diameter of 0.5 mm served as counter electrode. The reference electrode was a saturated calomel electrode (SCE). The counter electrode was carefully polished with abrasive paper (1500 mesh). The GCE was polished with alumina (Al_2O_3, 0.05 μm). Then the counter electrode and GCE were ultrasonically cleaned in turn with ethanol and deionized distilled water each for 5 min, respectively. Finally, they were dried in air before each experiment. All solutions (except for the solution containing VC) were deoxygenated by bubbling with dry argon for 10 min prior to each experiment. All experiments (except for the solution containing VC) were performed under slight argon overpressure. [Emim][$EtSO_4$] was used as supporting electrolyte for studying electrochemical polymerization of EDOT and electrochemical properties of PEDOT–$EtSO_4$ films. PEDOT–$EtSO_4$ films were electrosynthesized in 10 mM EDOT aqueous solution with different concentrations of [Emim][$EtSO_4$]. Cyclic voltammograms (CVs) of monomer and polymer were obtained at a potential scan rate of 100 mV s^{-1}. Electrochemical impedance spectroscopy (EIS) of PEDOT–$EtSO_4$ modified GCE was recorded at dc potential of 0.3 V vs. SCE, E_{ac}=10 mV, and the frequency range from 10 kHz to 0.1 Hz according to the potential (E_{dc}=0.3 V) of CVs of PEDOT–$EtSO_4$ modified GCE.

Electrochemical preparation of PEDOT–$EtSO_4$ matrix

The PEDOT–$EtSO_4$ matrix was prepared by one-step potentiostatical polymerization in 10 mM EDOT aqueous solution with different concentrations of [Emim][$EtSO_4$] at an applied potential of 1.10 V vs. SCE for 90 s on the surface of bare GCE (Scheme 1). Then the matrix was washed repeatedly with double-distilled deionized water to remove [Emim][$EtSO_4$] and EDOT. Electrochemical properties of PEDOT–$EtSO_4$ matrix were investigated in monomer-free aqueous solution with corresponding concentrations of [Emim][$EtSO_4$] by CVs and EIS.

Fabrication of PEDOT–$EtSO_4$/AO/Nafion electrode

Five microliters of 0.3 gL^{-1} AO was dip-coated on the surface of PEDOT–$EtSO_4$ modified GCE using a Finnpipette. After PEDOT–$EtSO_4$/AO modified GCE was dried in

air, 5 μL of 5% Nafion solution was dropped on the surface of AO layer to prevent possible enzyme molecules leakage and eliminate foreign interferences. Then PEDOT–$EtSO_4$/AO/Nafion modified GCE was allowed to air-dry at room temperature (Scheme 1), and the obtained PEDOT–$EtSO_4$/AO/Nafion modified GCE was stored in PBS at 4 °C when not used.

Measurements of VC electrochemical biosensor

The steady-state current response (I) of the fabricated biosensor for the amperometric detection of VC was carried out in VC standard solution at a working potential of 0.2 V vs. SCE. Different concentrations of VC ([VC]) standard solutions were prepared using 50 mM PBS (pH=6.5). The PEDOT–$EtSO_4$/AO/Nafion modified GCE served as the working electrode. All electrolysis cells were set in a thermostat, in which the temperature can be set constant at 25 °C. In addition, peak current densities of the fabricated biosensor for the voltammetric detection of VC was also recorded in PBS containing different [VC] at potential scan rate of 100 mV s^{-1}. In steady-state amperometric experiments, current–time (I–t) curves for the successive addition of VC standard solutions or sample solutions to a stirred cell with a stirring rate of 400 rpm at an operating potential of 0.2 V vs. SCE were recorded.

Working mechanism of VC electrochemical biosensor

The working mechanism of the fabricated biosensor for the bioelectrocatalytic oxidation of VC could be summarized as follows: the biosensor could facilitate the bioelectrocatalytic oxidation of VC to L-dehydroascorbic acid (DHA) and water (H_2O) in the presence of oxygen (O_2), and then the PEDOT–$EtSO_4$ acted as a direct electron-transfer mediator. AO molecules immobilized on the surface of PEDOT–$EtSO_4$ matrix could specifically recognize and bind to the two reactants VC and O_2. Then complex enzyme-catalytic process occurred, and a series of signals were accompanied and converted into electrical signals. Meanwhile, these electrical signals were captured by PEDOT–$EtSO_4$ matrix and transferred to GCE. Finally, they were detected and recorded by potentiostat–galvanostat under computer control. Nafion layer prevented the possible leakage of AO molecules and eliminated foreign interferences.

Determination of VC content in commercial juices

All commercial juices containing VC were purchased from a local supermarket. VC sample solutions were prepared from kinds of commercial juices containing VC and 50 mM PBS (pH=6.5). Finally, the content of different VC sample solutions was determined by amperometric and voltammetric methods using the fabricated VC electrochemical biosensor. Values were calculated by linear equation of the fabricated biosensor.

Apparatus

All electrochemical experiments were performed with a potentiostat–galvanostat (Model 263A; EG&G Princeton Applied Research). Samples were added with the Finn pipette (Labsystems, Helsinki, Finland). The pH value was measured with a Delta 320 pH meter (Mettler-Toledo Instrument, Shanghai, China). The temperature was controlled with a type HHS thermostat (Shanghai, China). EIS measurements were carried out using an Autolab Frequency Response Analyzer System (AUT30.FRA2-Autolab, Eco Chemie, BV, The Netherlands).

Results and discussion

Effect of [Emim][$EtSO_4$] concentration on electropolymerization of EDOT

To electrochemically synthesize the high-quality and high-performance PEDOT–$EtSO_4$ matrix of vitamin C electrochemical biosensor, the effect of [Emim][$EtSO_4$] concentration on electropolymerization of EDOT was investigated in an aqueous solution with different [Emim][$EtSO_4$] concentrations.

Chronoamperometry

EDOT was potentiostatically polymerized in aqueous solution with various [Emim][$EtSO_4$] concentrations at an applied potential of 1.1 V (Fig. 1). Current densities firstly ascended sharply for lower [Emim][$EtSO_4$]concentrations or declined for higher [Emim][$EtSO_4$] concentration, and then reached a plateau (Fig. 1 inset). This phenomenon was attributed to the electropolymerization mechanism of EDOT. Only a very limited amount of PEDOT–$EtSO_4$ films could be obtained on the bare GCE surface when molar ratios of [Emim][$EtSO_4$]/EDOT were lower than 1:4 or higher than 80:1, indicating that the concentration of [Emim][$EtSO_4$] strongly influenced the electrosynthesis of PEDOT–$EtSO_4$ films. The concentration of dissociated ions in aqueous solution was very low when the concentration of [Emim][$EtSO_4$] was lower, which would adversely affect the electropolymerization of EDOT due to the lower concentration of the supporting electrolyte. The viscosity of [Emim][$EtSO_4$] increased with increasing the concentration of [Emim][$EtSO_4$]. As a result, the formation of $EDOT^{+\bullet}$ and PEDOT–$EtSO_4$ films and diffusion processes would be hindered during the formation of PEDOT–$EtSO_4$ films

(Scheme 1). In addition, PEDOT–$EtSO_4$ films were easily prepared at molar ratios of [Emim][$EtSO_4$] to EDOT between 1:1 and 40:1, revealing that the effect of the concentration of [Emim][$EtSO_4$] on the electropolymerization of EDOT could be attributed to structural features of [Emim][$EtSO_4$] aqueous solution [30]. Isolated water molecules and isolated ions or small ion clusters are unsuitable for electrochemical preparation of PEDOT–$EtSO_4$ films at very low or high concentration of [Emim][$EtSO_4$], while chain-like water aggregates and bicontinuous system are beneficial to the electrosynthesis of PEDOT–$EtSO_4$ films in aqueous solution with the appropriate [Emim][$EtSO_4$] concentration. Therefore, an optimal molar ratio of 10:1 was chosen for the electrosynthesis of PEDOT–$EtSO_4$ films and used in the following experiment based on results presented above and a series of comparison experiments.

In addition, the thickness of PEDOT–$EtSO_4$ matrix was also studied in the aqueous solution with different [Emim][$EtSO_4$] concentrations. A set of current transients were shown in Fig. 1 inset during electropolymerization of EDOT containing different concentrations of [Emim][$EtSO_4$]. Two or more stages were clearly observed at different concentrations of [Emim][$EtSO_4$]. The initial stage in electropolymerization of EDOT was a combination of instantaneous 2D and 3D mechanisms since electropolymerization of EDOT was under charge transfer control rather than diffusion. In the later stage in electropolymerization of EDOT, layer-by-layer growth mode was in accordance with the Stranski–Krastanov model [49–51]. It is an important feature that the layer-by-layer growth mode demonstrates the electrochemical feasibility of ultrathin PEDOT films, and this plays an important role in modern biosensors [49–51]. In comparison

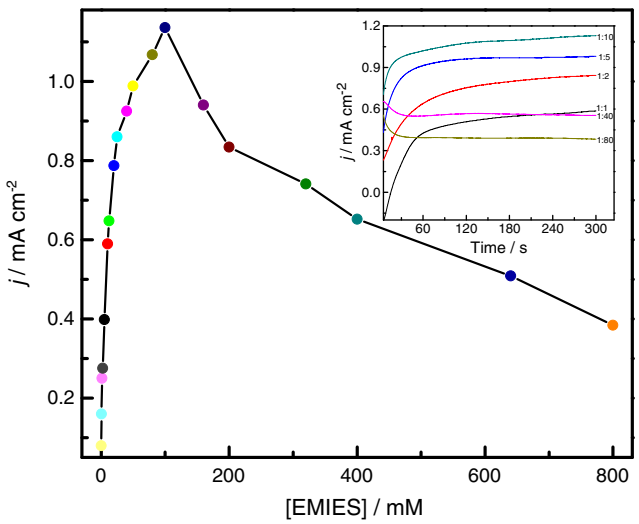

Fig. 1 The potentiostatical polymerization of EDOT in different concentrations of [Emim][$EtSO_4$] aqueous solutions. *Inset*: chronoamperometric curves recorded with molar concentration ratios of EDOT/[Emim][$EtSO_4$]=1:1, 1:2, 1:5, 1:10, 1:40, and 1:80

with electropolymerization of EDOT with different concentrations of [Emim][$EtSO_4$], the nucleation process took least time at approximately 100 mM [Emim][$EtSO_4$], further indicating that the electropolymerization of EDOT was greatly influenced by the viscosity and concentration of [Emim][$EtSO_4$]. The thickness of PEDOT–$EtSO_4$ films was controlled by the total charge passed through the cell, which was read directly from *I–t* curves displayed on a computer. In our previous studies [51], the thickness of films directly influenced the performance of biosensor based on PEDOT matrix. Therefore, a deposition time of 90 s was selected for subsequent experiments.

Cyclic voltammetry

EDOT was electrochemically polymerized by successive CVs between −0.95 V and 1.15 V vs. SCE in different concentrations of [Emim][$EtSO_4$] (Fig. 2). As shown in Fig. 2a and f, the successive CVs of EDOT exhibited similar characteristics at very low or high concentrations of [Emim][$EtSO_4$]. The increase of redox current densities was not obvious with increasing the cycle numbers of potential scan, implying that the electropolymerization of EDOT was significantly influenced at very low or high concentrations of [Emim][$EtSO_4$]. The main reason resulted in the phenomenon was in agreement with that mentioned above. The increase of redox current densities (Fig. 2b–e) was very clear with increasing the cycle numbers of potential scan when concentrations of [Emim][$EtSO_4$] were in the range 10 to 400 mM, suggesting that the amount of conducting polymers electrodeposited on the surface of bare GCE increased. Moreover, cathodic peaks at about −0.5 V were very visible, and clear broad anodic waves appeared between 0 and 0.8 V. However, cathodic peaks gradually disappeared and anodic waves significantly weakened (Fig. 2e–f) when the concentration of [Emim][$EtSO_4$] increased gradually, which was similar with our reports [51]. This phenomenon was related to the electropolymerization mechanism of EDOT of physicochemical properties of [Emim][$EtSO_4$] (Scheme 1). Successive CVs of EDOT in Fig. 2c and d showed better characteristics in comparison with other successive CVs of EDOT in Fig. 2, indicating that the electropolymerization of EDOT easily proceeded at appropriate concentration range, which was in accordance with electropolymerization of EDOT in ILs microemulsion [46]. In addition, visual inspection revealed that large amounts of PEDOT–$EtSO_4$ films were obtained on the surface of bare GCE. The molar ratios of [Emim][$EtSO_4$]/EDOT were 10:1, and the successive CVs of EDOT in Fig. 2d illustrated best characteristics, which further indicated that a molar ratio of 10:1 was deemed optimal and used in subsequent experiments.

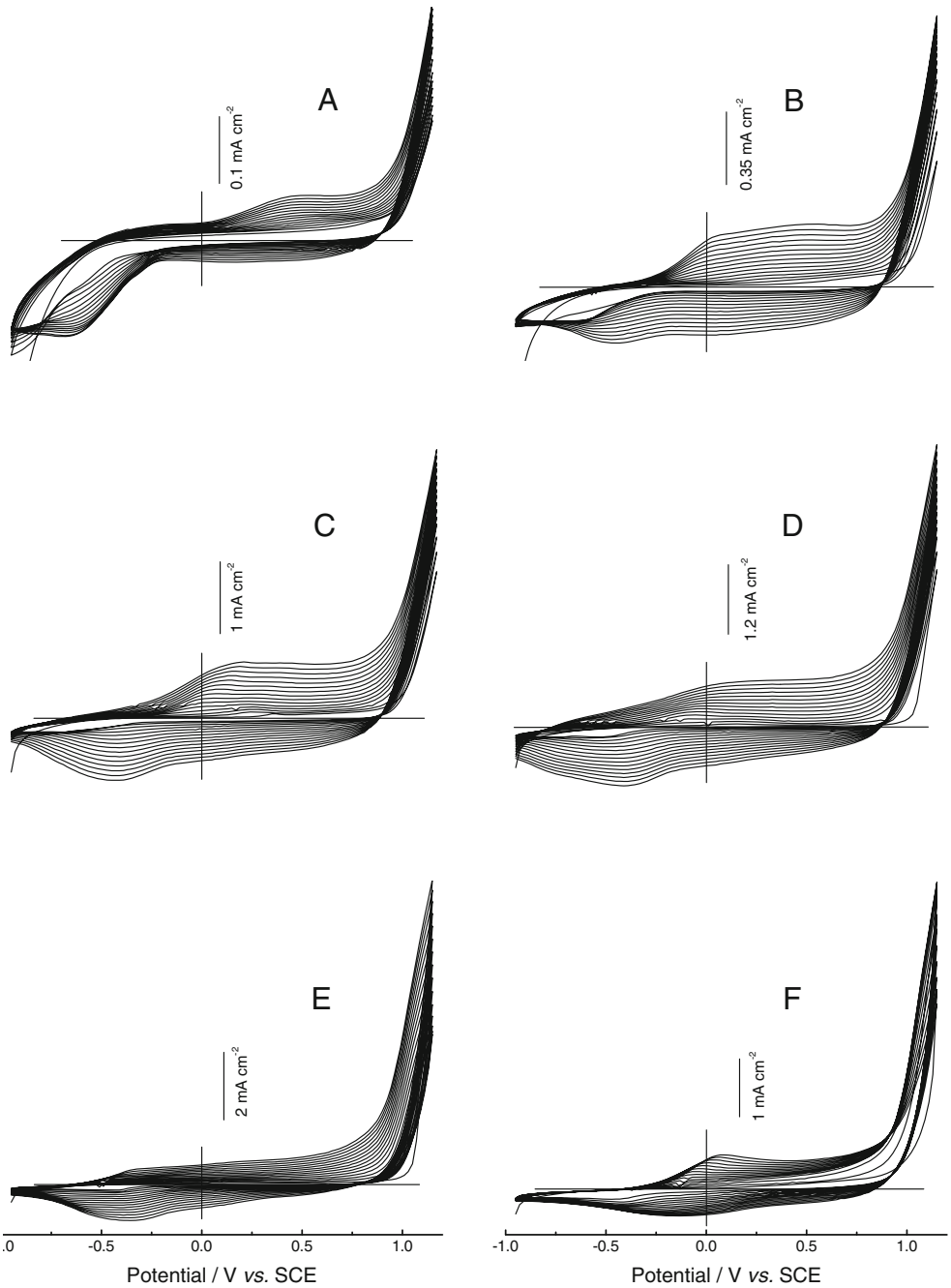

Fig. 2 Successive CVs of EDOT at molar concentration ratios of [Emim][$EtSO_4$]/EDOT=**a** 4:1, **b** 1:1, **c** 1:5, **d** 1:10, **e** 1:40, **f** 1:80

Electrochemical behaviors of PEDOT–$EtSO_4$ films

Electrochemical properties of the electrode matrix directly influenced the performance of the electrochemical biosensor, hence electrochemical behaviors of the prepared PEDOT–$EtSO_4$ matrix were also studied in a monomer-free aqueous solution with corresponding [Emim][$EtSO_4$] concentration.

Cyclic voltammetry of PEDOT–$EtSO_4$ films

Electrochemical behaviors of PEDOT–$EtSO_4$ films deposited potentiostatically in different concentrations of [Emim][$EtSO_4$] were investigated in monomer-free aqueous solution with corresponding [Emim][$EtSO_4$] concentration (Fig. 3a). Cyclic voltammetric curves did not show any clear oxidation or reduction peaks in the potential range −0.3 to 0.3 V, but merely a rectangle-like shape (Fig. 3a), indicating good capacitive characteristics of PEDOT–$EtSO_4$ films. In addition, values of voltammetric charges (Q_{CV}) and voltammetric capacitances (C_{CV}) at E_{dc}=0.3 V for obtained PEDOT–$EtSO_4$ films are listed in Table S1. A concentration of 100 mM seems to be a turning point. Q_{CV} and C_{CV} values gradually increased with increasing the concentration of [Emim][$EtSO_4$] in the range of 12.5 to 100, which was

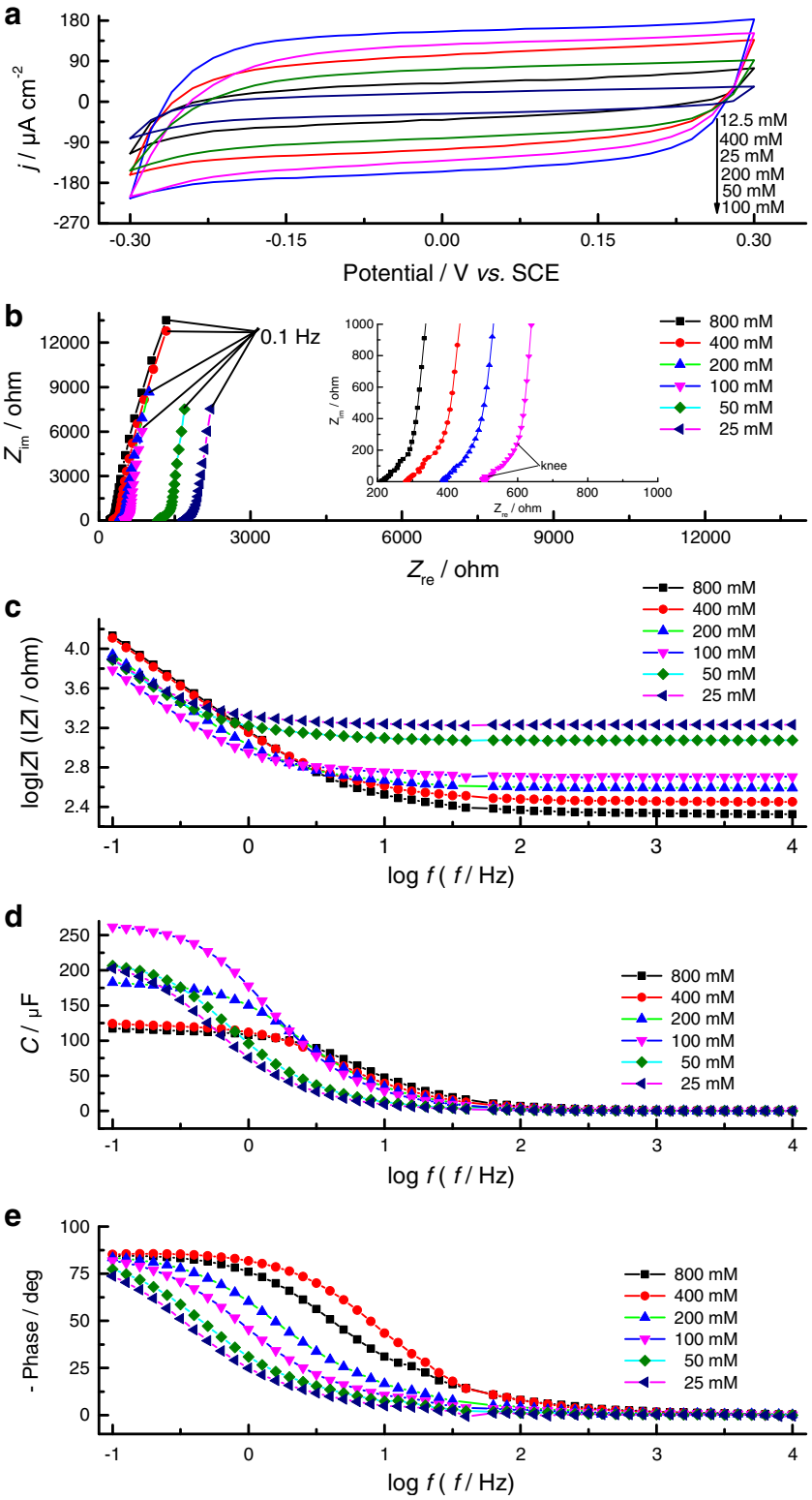

Fig. 3 Electrochemical behaviors of PEDOT modified GCE, including **a** CVs, **b** Bode plots, and **c** Nyquist plots. PEDOT films were potentiostatically synthesized in corresponding concentrations of [Emim][$EtSO_4$]

associated with the doping level of PEDOT films. Q_{CV} and C_{CV} values gradually decreased with increasing concentration of [Emim][$EtSO_4$] in the range of 100 to 400 mM, which might influence the doping level of PEDOT films. In addition, PEDOT–$EtSO_4$ films were continuously scanned in monomer-free aqueous solution with 100 mM [Emim][$EtSO_4$] at the potential scan rate of 100 mV s^{-1}; almost unchanged current densities of polymer films revealed that obtained PEDOT–$EtSO_4$ films have good electrochemical activity and stability, which is very

beneficial to the design and application of biosensors. Cyclic voltammetric responses of PEDOT films electrosynthesized in [Emim][$EtSO_4$] aqueous solution also compared with that obtained in the traditional supporting electrolyte aqueous solution such as PSSNa and $LiClO_4$ (Fig. S1A); anodic and cathodic peak current densities of PEDOT–$EtSO_4$ films were obviously increased. Enhanced peak current densities indicated the high electrical conductivity of dopant ($EtSO_4^-$) in PEDOT films. Moreover, the peak-to-peak separation of 100 mV of PEDOT–$EtSO_4$ was much lower than that of 122 mV of PEDOT–PSS and PEDOT–ClO_4. The smaller peak-to-peak separation indicated a faster electron transfer of the dopant ($EtSO_4^-$) in PEDOT films.

Impedance plots of PEDOT–$EtSO_4$ films

EIS is an effective method for probing features of the surface-modified electrode. Therefore, the impedance spectra of the PEDOT–$EtSO_4$ modified GCE was studied in the [Emim][$EtSO_4$] concentration range of 6.25 to 800 mM (Fig. 3b–e). Bode and Nyquist plots of the as-prepared PEDOT–$EtSO_4$ modified GCE were recorded by EIS. All Bode plots of the PEDOT–$EtSO_4$ modified GCE demonstrated the frequency dependence of the magnitude $|Z|$ and phase angle (Φ) (Fig. 3b, e) and were separated into three regions: the high-frequency region, medium-frequency region, and low-frequency region. Nyquist plots are shown in Fig. 3b with the real part (Z_{re}) on the X-axis and the imaginary part (Z_{im}) on the Y-axis. From all Nyquist plots of PEDOT–$EtSO_4$ modified GCE (Fig. 3b), two distinct regions can be seen: a Warburg diffusion impedance with a characteristic 45° slope at high frequency range and a nearly vertical line which represents a pure capacitive region in the low frequency range, which was similar with Nyquist plots of most PEDOT films reported in previous studies [50, 52].

In the high-frequency region in Bode plots, $|Z|$ value was weakly dependent on frequency, and the phase angle was near zero (Fig. 3c). Moreover, The $|Z|$ value decreased with the increase in [Emim][$EtSO_4$] concentration, which was related to the doped level of anions ($EtSO_4^-$). The ionic conductivity of ILs increased with increasing ILs concentration in lower concentration range [46], which could decrease ionic resistance of PEDOT–$EtSO_4$ films and improve the conductivity of polymer films. The high-frequency region in Nyquist plots, a Warburg-like region, was presented by a line inclined at approximately 45° in complex plane; this was similar to previous reports on EIS of oxidized PEDOT film electrodes [54, 55]. The high-frequency intersection with the Z_{re} axis depends strongly on the concentration of [Emim][$EtSO_4$] and is consequently determined by the solution resistance (R_s). R_s (Table 1) was found to be inversely proportional to the concentration of the supporting electrolyte ([Emim][$EtSO_4$]), which was in good agreement with the literature [54].

In the middle-frequency range, "knee frequency", the crossing of the high-frequency inclined line with the low-frequency vertical line divided Nyquist plots into the high- and low-frequency region (Fig. 3b inset). Knee frequencies of PEDOT–$EtSO_4$ modified GCE were derived approximately from the enlarged Nyquist plots in Fig. 3b inset and are listed in Table 1. Knee frequencies increased with the increase in [Emim][$EtSO_4$] concentration, and higher knee frequencies revealed that PEDOT–$EtSO_4$ films had faster charge transfer. As can be seen from log$f$−C plots in Fig. 3d, the whole capacitance was reached below "knee frequency"; the capacitance strongly depended on the frequency for higher values.

The region where log f−log $|Z|$ plots displayed a slope close to −1 can be regarded as the low-frequency region (Fig. 3c). The capacitance (C) of conducting polymer films was calculated according to the equation $C = (2\pi f Z_{im})^{-1}$, where f is the frequency of the impedance and Z_{im} is the imaginary part of the impedance [50, 53]. The characterization of near −1 slope in Fig. 3c indicated that this region was a typical capacitive behavior (Fig. 3d).

The low-frequency region in Nyquist plots was related to the capacitance of the PEDOT–$EtSO_4$ modified GCE (corresponding to low-frequency region of Bode plots). The Z_{im} of all impedance sharply increased and all plots tended to a vertical line at the low-frequency region, indicating a good capacitance behavior. Maximum capacitance values (C_{max}) were calculated from Z_{im} value at the lowest frequency (0.1 Hz) using the equation mentioned above. The data are presented in Table 1; C_{max} values gradually increased with increasing concentration of [Emim][$EtSO_4$] when the concentration of [Emim][$EtSO_4$] was less than 100 mM, while C_{max} values gradually decreased with increasing concentration of [Emim][$EtSO_4$] when the concentration of [Emim][$EtSO_4$] exceeded 100 mM (Fig. 3d), indicating that a concentration of 100 mM was a turning point. The main reason was relative to the doping level and viscosity of [Emim][$EtSO_4$]. In addition, C_{max} values were also in accordance with that in EIS capacitance (C_{EIS}), which was directly read from an Autolab Frequency Response Analyzer. However, the variation trend between Z_{im} and the [Emim][$EtSO_4$] concentration was contrary to the variation trend between C_{max} and [Emim][$EtSO_4$] concentration according to the equation mentioned above. Similarly, Z_{im}, Z_{re}, and $|Z|$ followed a similar trend (Table 1). These results also indicated that 100 mM [Emim][$EtSO_4$] was the optimal concentration, and obtained PEDOT–$EtSO_4$ films had better electrochemical properties in comparison with other concentrations of [Emim][$EtSO_4$].

The ionic resistance (R_{ion}) of PEDOT–$EtSO_4$ films was calculated by $R_{ion} = 3\left[Z'_{low} - Z'_{high}\right]$, where Z'_{low} is the low-

Table 1 Bode and Nyquist plots of the PEDOT–$EtSO_4$ matrix recorded using the Autolab Frequency Response Analyzer System

[Emin][$EtSO_4$] (mM)	800	400	200	100	50	25
Z_{re} (kΩ)	1.33	1.33	0.994	0.856	1.694	2.216
Z_{im} (kΩ)	13.59	12.86	8.723	6.089	7.705	7.861
C_{EIS} (μF)	117.2	123.9	182.5	261.5	206.7	202.6
Knee (Hz)	10	6.30	3.98	3.16	1.26	1
Φ	−84.38°	−84.06°	−83.46°	−81.91°	−77.3°	−73.62°
R_s (Ω)	211.6	281.5	388.3	506.1	1197.1	1689.5
Z'_{low} (Ω)	251.3	346.1	464.6	593.5	1372.8	1882.4
R_{ion} (Ω)	119.1	193.8	228.9	262.2	527.1	578.7
C_{max} (μF)	117.75	124.53	183.74	264.2	211.86	211.13
$\|Z\|$ (kΩ)	13.52	12.79	8.666	6.028	7.526	7.542

The PEDOT–$EtSO_4$ matrix was prepared by one-step potentiostatical polymerization in 10 mM EDOT aqueous solution with different concentrations of [Emim][$EtSO_4$] at an applied potential of 1.10 V vs. SCE for 90 s on the surface of bare GCE. EIS results of PEDOT–$EtSO_4$ modified GCE were recorded at dc potential of 0.3 V vs. SCE, E_{ac}=10 mV, and the frequency range from 10 kHz to 0.1 Hz. Z_{re}, Z_{im}, C_{EIS}, $|Z|$, and Φ were obtained from Autolab Frequency Response Analyzer at the frequency of 0.1 Hz

frequency limiting resistance, which was obtained by the real axis intercept of a linear regression through the low-frequency data; Z'_{high} is the high-frequency intercept with the real impedance axis [55]. It can be seen that the length of the Warburg-like region $\left(\sim Z'_{low} - Z'_{high}\right)$ decreased with increasing concentration of [Emim][$EtSO_4$] (Table 1), indicating that the R_{ion} of PEDOT–$EtSO_4$ films increased with decreasing concentration of the supporting electrolyte ([Emim][$EtSO_4$]]). The lower R_{ion} suggested that the ion transport in PEDOT–$EtSO_4$ films was much faster. In addition, PEDOT–$EtSO_4$ films obtained in 100 mM [Emim][$EtSO_4$] aqueous solution has lower resistance according to results mentioned above and presented in Table 1, revealing that the as-prepared PEDOT–$EtSO_4$ matrix in IL/W containing 100 mM [Emim][$EtSO_4$] had good electrochemical properties. Moreover, the lower R_{ion} also implied that the as-prepared PEDOT–$EtSO_4$ films had higher conductivity.

To further confirm electrochemical properties of obtained PEDOT–$EtSO_4$ films, Nyquist and Bode plots of PEDOT–$EtSO_4$ films also compared with that of PEDOT films obtained in the traditional supporting electrolyte such as PSSNa and $LiClO_4$ (Fig. S1B and C). In the high-frequency region in Bode plots, the $|Z|$ value of PEDOT–$EtSO_4$ modified GCE at phase angle close to zero was minimum (Fig. S1B), suggesting that [Emim][$EtSO_4$] possessed higher ionic conductivity than PSSNa and $LiClO_4$, which decreased the R_{ion} of PEDOT modified GCE, indicating that the obtained PEDOT–$EtSO_4$ films had better conductivity due to lower resistance. Furthermore, Bode plots also revealed that PEDOT–$EtSO_4$ had maximal capacitance and Φ. In Nyquist plots of PEDOT–$EtSO_4$ modified GCE (Fig. S1C), it was found that the resistance of PEDOT–$EtSO_4$ modified GCE in 0.1 M KCl aqueous solution containing 5 mM $Fe(CN)_6^{3-/4-}$ redox couple was significantly lower than that PEDOT–PSS (PEDOT–ClO_4) modified GCE in 0.1 M KCl aqueous solution containing 5 mM $Fe(CN)_6^{3-/4-}$ redox couple (Table S2 and Fig. S1C); these could be ascribed to the effect of the ionic conductivity on doping ions. Moreover, in CVs of PEDOT–$EtSO_4$ modified GCE, the reduced peak-to-peak separation and enhanced voltammetric peak current densities were observed in comparison with PEDOT–PSS (PEDOT–ClO_4) modified GCE (Fig. S1A), suggesting that the PEDOT–$EtSO_4$ modified GCE exhibited a fast electron transfer. Hence, the prepared conducting PEDOT–$EtSO_4$ matrix with good electrochemical properties would be beneficial for the subsequent development and application of biosensing devices.

Detection of VC

Voltammetric detection of VC

Figure 4 shows peak current densities of the biosensor for the bioelectrocatalytic oxidation of VC. It could be seen that the bioelectrocatalytic oxidation of VC began to appear from −0.05 V and reached a maximum value at approximately 0.15 V. Moreover, peak current densities gradually increased with increasing the [VC], suggesting that the fabricated biosensor possessed an excellent bioelectrocatalytic performance for the bioelectrocatalytic oxidation of VC. In addition, the oxidation peak potential of the biosensor for the bioelectrocatalytic oxidation of VC was gradually shifted to a less-positive potential when [VC] was higher than 1 mM, which ascribed to the consumption of dissolved O_2 in surrounding enzymes.

The linear relationship between peak current densities and [VC] is shown in Fig. 4 inset. Obviously, the value of peak current densities linearly increased with increasing the [VC], revealing that the unknown content of VC could be

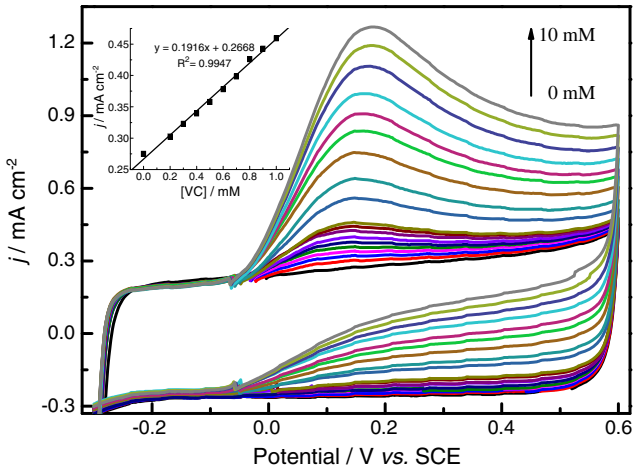

Fig. 4 The oxidation peak current of the fabricated biosensor in PBS containing different [VC], an increment in [VC] is 0.1 mM in concentration range from 0.2 to 1 mM and 1 mM in concentration range from 2 to 10 mM, respectively. *Inset*: the linear portion of [VC] range

successfully detected using the fabricated biosensor. Moreover, the biosensor showed a linear range up to 1 mM (y=0.196x+0.2668, R^2=0.9947) with a sensitivity of 191.6 mA M^{-1} cm^{-2} (from the slope of the linear part in Fig. 4 inset). The limit of detection (LOD) and limit of quantification (LOQ) were calculated using the following equations:

$$\mathrm{LOD} = 3s/m \qquad \mathrm{LOQ} = 10s/m$$

where s is the standard deviation of the peak current of the lowest concentration of the linearity range and m is the slope of linear equation in Fig. 4 inset. LOD and LOQ were calculated as 0.0742 mM and 0.2474 mM, respectively. These results indicated that the fabricated biosensor had an excellent performance for the bioelectrocatalytic oxidation of VC. Oxidation peak densities displayed a gradual deviation from linearity when [VC] was higher than 1 mM, possibly because insufficient amounts of the dissolved O_2 due to the consumption of the dissolved O_2 in surrounding enzyme.

Amperometric determination of VC

Working potential

Changes in current responses of the fabricated biosensor at different working potentials are shown in Fig. S2. The working potential of the biosensor is in a range of −0.1 to 0.2 V; I increased rapidly in the beginning, and then reached a steady state within 2 s, which indicated that the current response of the biosensor was controlled by kinetics of the enzyme-catalyzed reaction and electrochemical processes. However, current responses became almost constant when the working potential varied from 0.2 to 0.5 V, indicating that the biosensor response was limited by the diffusion of substrates and products.

The relationship between current responses and working potentials indicated that very little working potential dependence was observed at potential above 0.2 V. A lower working potential was desirable for avoiding the interference of reducing agents in real samples. Therefore, the working potential of 0.2 V was selected as the optimal working potential of the as-fabricated biosensor for subsequent experiments. Moreover, the working potential was significantly lower than that in previous reports (Table S3).

Current–time curves

The bioelectrocatalytic performance of the fabricated biosensor towards the oxidation of VC was investigated by chronoamperometry. Figure 5 shows I–t plots of the biosensor in PBS containing various [VC] at the working potential of 0.2 V. Obviously, current responses gradually increased with increasing the [VC], revealing that this method is suitable for detecting the unknown content of VC. I–[VC] relationship revealed that there was a wide linearity of the current response versus [VC] from 8.0×10^{-7} to 1×10^{-3} M (y=0.1048x+0.0009, R^2=0.9997), with a sensitivity of 104.8 mA M^{-1} cm^{-2}, LOD of 0.147 μM, and LOQ of 0.487 μM. In addition, I–t curves of the biosensor exhibited a fast response time (approximately 2 s). However, the response time gradually lengthened at higher [VC], and the curve exhibited a gradual deviation from linearity. The main reason for this phenomenon is the consumption of dissolved O_2 amounts resulting in the insufficient O_2 dissolved in surrounding enzyme, and AO molecules became progressively saturated with increasing the concentration of substrate. In contrast to previous reports, the analytical performance of the AO-based biosensor is listed in Table S3. From these results, we could see that the fabricated biosensor had wider linear range, faster current response, lower detection limit, and higher sensitivity, which ascribed to superior electrochemical properties of the prepared conducting PEDOT–$EtSO_4$ matrix.

Performance of VC electrochemical biosensor

Bioaffinity and bioactivity

The bioaffinity of the fabricated biosensor was obtained by Lineweaver–Burk plots in Fig. 6a. Parameters were calculated by the Lineweaver–Burk equation as follows:

$$\frac{1}{I} = \frac{K'_{\mathrm{mapp}}}{I'_{\mathrm{max}}}\frac{1}{[\mathrm{VC}]} + \frac{1}{I'_{\mathrm{max}}}$$

K'_{mapp} (the apparent Michaelis–Menten constant) and I'_{max} (the apparent maximum steady–state current response) values were calculated by the equation above. After linear

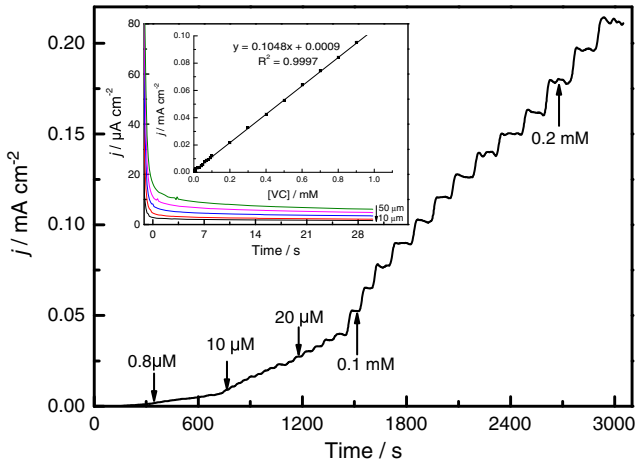

Fig. 5 *I–t* plots of the fabricated biosensor for addition of successive aliquots of VC in PBS under optimized experimental conditions. *Inset*: current responses of the biosensor for the bioelectrocatalytic oxidation of VC in different [VC] and the linear portion of [VC] range

regression, an equation of the form $y–A+Bx$ was obtained. The inverse of A is I'_{max}, as at that point, x is zero; whereas K'_{mapp} is calculated as $B\ (A)^{-1}$, as at that point, y is zero. K'_{mapp} and I'_{max} values were 8.688 mM and 1.051 mA cm^{-2}, respectively. These values were significantly lower than that in our previous reports [50, 51]. Michaelis–Menten constant

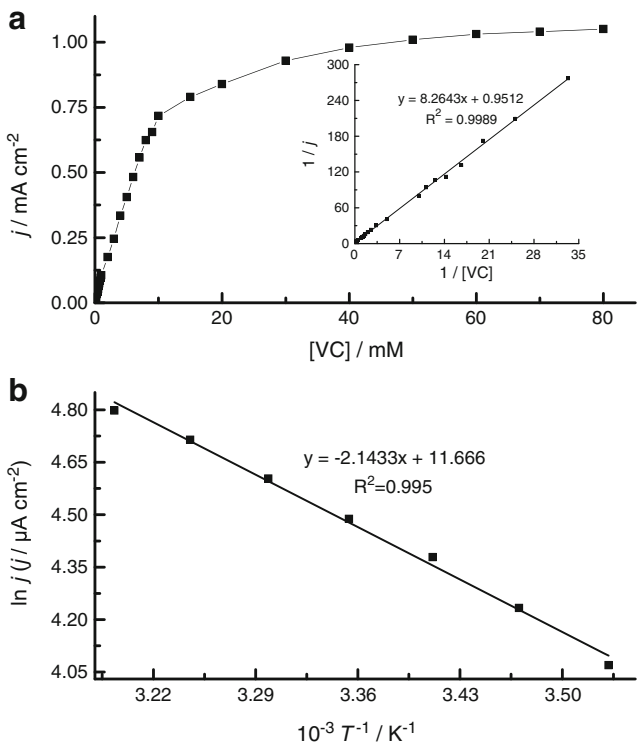

Fig. 6 The bioaffinity and bioactivity of the fabricated biosensor and *I*–[VC] relationship of the biosensor. *Inset*: Lineweaver–Burk plots of the biosensor under optimized experimental conditions (**a**), the determination of E'_a of the biosensor (**b**)

is a measure of enzymatic affinity for substrates and corresponds to the concentration of substrate at 1/2 V_{max}. It is inversely proportional to the enzymatic affinity for its substrates. Therefore, the lower value of K'_{mapp} indicated the high bioaffinity of the fabricated biosensor to substrates.

In addition, the apparent activation energy (E'_a) of the fabricated biosensor was obtained by ln I vs. $1/T$ graph in Fig. 6b. The ln I vs. $1/T$ graph depicts the relationship between the Napierian logarithm of I and the inverse of the temperature. The value of E'_a was calculated by the Arrhenius equation as follows:

$$\ln k = \ln k_0 - \frac{E'_a}{RT} \Rightarrow \ln I = \ln I_0 - \frac{E'_a}{RT}$$

After linear regression, an equation of type $y=A+Bx$ was obtained, and then the apparent activation energy was

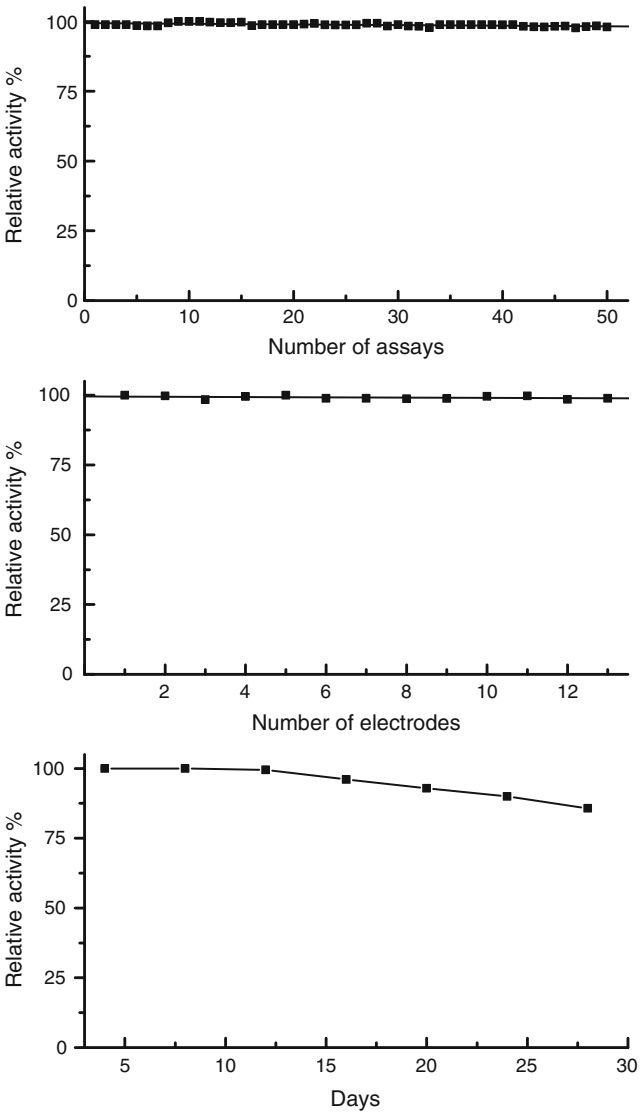

Fig. 7 The stability of the fabricated biosensor: repeatability (**a**), reproducibility (**b**), and storage stability(**c**)

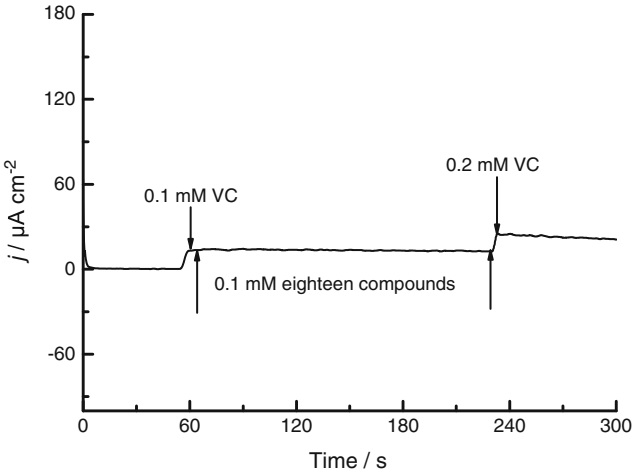

Fig. 8 Current responses of the fabricated biosensor were recorded in constant VC solutions containing 1 mM different substances

calculated from $E_a^{'} = BR$. The value of $E_a^{'}$ was 17.819 kJ M^{-1}, which was much lower than that in previous reports [51]. The lower value of $E_a^{'}$ meant that PEDOT–$EtSO_4$/AO/Nafion electrode possessed higher bioactivity and bioaffinity towards substrates, which was in agreement with the lower value of $K_{mapp}^{'}$.

Stability

The repeatability and reproducibility of the biosensor are very important parameters when testing its analytical performance. However, biologically active species have limited stability, especially when they are removed from native microdomains, and immobilized in the non-native matrix. Thus, the reproducibility and repeatability of the fabricated biosensor should be evaluated.

The repeatability of the fabricated biosensor in terms of repetitive use in PBS containing 0.5 mM VC is presented in Fig. 7a. The coefficient of variation was 0.476% for 50 successive assays, showing a fairly good repeatability of PEDOT–$EtSO_4$/AO/Nafion electrode.

The reproducibility of the fabricated biosensor was evaluated via the comparison of the current response of the prepared 13 PEDOT–$EtSO_4$/AO/Nafion electrodes. These electrodes were tested independently for current responses of VC bioelectrocatalytic oxidation (Fig. 7b), providing a coefficient of variation value of 0.563%. Good results indicated an efficient and reproducible immobilization process for AO molecules on the surface of conducting PEDOT–$EtSO_4$ matrix. The excellent repeatability and reproducibility demonstrated the high stability of the as-fabricated biosensor and the controllable process for the quantity of enzyme.

The storage stability or shelf-life of the fabricated biosensor was also assessed by its storage and operational efficiency. To determine the storage stability or shelf-life of the as-fabricated biosensor, measurements were carried out periodically every day in the first 2 weeks and every 4 days in the second 2 weeks. The biosensor was used for only this purpose and it was stored in PBS at 4 °C. No loss of the bioactivity in current response was observed for 11 days and decreased approximately 6% after being stored for 20 days (Fig. 7c). Moreover, 85.71% of bioactivity still remained even after stored for 4 weeks. The high stability of the as-fabricated biosensor also suggested that the as-prepared conducting PEDOT–$EtSO_4$ matrix as enzyme carriers has high stability. [Emim][$EtSO_4$] and Nafion provide the biocompatible environment for biologically active AO macromolecules.

Specificity

Different substances such as carbohydrates, amino acids, organic acids, and alcohols were used to test the specificity of the biosensor. *I–t* curve in Fig. 8 showed that the addition of 0.1 mM VC caused a noticeable change in current response, while the successive addition of 1 mM 18

Table 2 The content of VC in commercial juices determined using the fabricated PEDOT–$EtSO_4$/AO/Nafion biosensor, and VC sample solutions containing 50 mM PBS (pH=6.5) prepared from kinds of commercial juices with VC content

Commercial drinks	[VC] (mg/mL)	[VC] by amperometric method (mg/mL)[a]			[VC] by voltammetric method (mg/mL)[a]		
		Mean	RSD %	Recovery %	Mean±SD	RSD %	Recovery %
Fruit blend	0.1	0.094	0.617	94	0.093	2.052	93
Vitamin water	0.2	0.195	0.468	97.5	0.192	1.208	96
Lemon juice	0.225	0.216	0.283	96	0.212	1.025	94.222
Mizone	0.2	0.194	0.391	97	0.193	1.105	96.5
Orange juice	0.13	0.124	0.395	95.385.	0.123	1.108	94.65

RSD relative standard deviation

[a] Average value of five replications

compounds (glucose, fructose, sucrose, L-glutamic acid, L-aspartic acid, DL-alanine, L-glycine, inositol, DL-malic acid, oxalic acid, citric acid, edetic acid, thiamine, nicotinic acid, mannite, sorbierite, melamine, and urea) did not cause an significant change in current response, revealing that the as-fabricated biosensor has good anti-interference ability, and AO molecules and Nafion film provide good selectivity for the determination of VC. In addition, the current response or peak current of the as-fabricated biosensor was also determined in PBS containing a constant VC and 18 compounds with the concentrations of 1×10^{-4} and 1×10^{-3} M, respectively. Results are listed in Table S4; these substances did not cause significant interference in current responses of the fabricated biosensor, further indicating that the as-fabricated biosensor had good specificity.

Determination of VC in commercial juices

To establish the viability of the biosensor for real sample analysis, Table 2 gives analytical results for the determination of VC in commercial juices. Values obtained by the fabricated biosensor were in good agreement with that given by the manufacturer, which demonstrated the feasibility and reliability of the present method. Therefore, good results indicated that the fabricated biosensor could be employed to the determination and analysis of VC in real samples.

Conclusion

The conducting PEDOT–$EtSO_4$ matrix with good electrochemical properties was easily prepared by the one-step potentiostatical polymerization of EDOT in [Emim][$EtSO_4$]-in-water with the appropriate concentration of [Emim][$EtSO_4$]. CVs and EIS results indicated that the obtained PEDOT–$EtSO_4$ matrix had high conductivity and stability. AO molecules were successfully immobilized on the surface of the resulting PEDOT–$EtSO_4$ matrix by the high selective Nafion layer. The fabricated PEDOT–$EtSO_4$/AO/Nafion biosensor could be employed for direct, fast, and specific determination of VC in commercial juices using amperometric and voltammetric methods. In addition, the biosensor also exhibited high bioaffinity, good bioactivity, wide linear range, fast current response, low detection limit, pronounced sensitivity, high stability, and good specificity. The good performance of the fabricated biosensor and good results for the determination of VC in commercial juices will benefit agricultural application in real samples in the near future, and the obtained conducting PEDOT–$EtSO_4$ matrix as immobilization matrix of biologically active species also provides a promising platform for the development and application of biosensing devices.

Acknowledgments NSFC (50963002, 51073074), Key Projects in the National Science & Technology Pillar Program in the Eleventh Five-year Plan Period (2006BAD02A04, 2006BAD01A01), Jiangxi Provincial Department of Science and Technology (2006BAD01A01-2-5), Jiangxi Provincial Department of Education (GJJ11590, GJJ10678), Natural Science Foundation of Jiangxi Province (2010GZH0041), and Key Laboratory of Photochemical Conversion and Optoelectronic Materials, TIPC, CAS, are acknowledged for their financial support.

References

1. Mazurkiewicz JH, Innis PC, Wallace GG, MacFarlane DR, Forsyth M (2003) Conducting polymer electrochemistry in ionic liquids. Synth Met 135:31–32
2. Don B, Xu JK, Zheng LQ (2009) Ionic liquids for the electrosyntheses of conducting polymers. Prog Chem 21:1792–1799
3. Lu J, Yan F, Texter J (2009) Advanced applications of ionic liquids in polymer science. Prog Polym Sci 34:431–448
4. Shiddiky MJA, Torriero AAJ (2010) Electrochemical properties and applications of ionic liquids. Nova Science, USA
5. Lu W, Fadeev AG, Qi B, Smela E, Mattes BR, Ding J, Spinks GM, Mazurkiewicz J, Zhou D, Wallace GG (2002) Use of ionic liquids for π-conjugated polymer electrochemical devices. Science 297:983–987
6. Wei D, Ivaska A (2008) Applications of ionic liquids in electrochemical sensors. Anal Chim Acta 607:126–135
7. Wasserscheid P, Hal RV, Bösmann A (2002) One-pot, three-component synthesis of α-aminophosphonates catalyzed by acyclic acidic ionic liquids. Green Chem 4:400–404
8. Cammarata L, Kazarian SG, Salter PA, Welton T (2001) Molecular states of water in room temperature ionic liquids. Phys Chem Chem Phys 3:5192–5200
9. Holbrey JD, Reichert WM, Swatloski RP, Broker GA, Pitner WR, Seddon KR, Rogers RD (2002) Efficient, halide free synthesis of new, low cost ionic liquids: 1, 3-dialkylimidazolium salts containing methyl-and ethyl-sulfate anions. Green Chem 4:407–413
10. Lin PY, Soriano AN, Leron RB, Li MH (2011) Measurements and correlations of electrolytic conductivity and molar heat capacity for the aqueous ionic liquid systems containing [Emim][$EtSO_4$] or [Emim][CF_3SO_3]. Exp Therm Fluid Sci 35:1107–1112
11. Alvarez VH, Mattedi S, Aznar M (2011) Isobaric (vapor + liquid) equilibria of 1-ethyl-3-methylimidazolium ethylsulfate plus (propionaldehyde or valeraldehyde): experimental data and prediction. J Chem Thermodyn 43:895–900
12. Harrar A, Zech O, Hartl R, Bauduin P, Zemb T, Kunz W (2011) [emim][$etSO_4$] as the polar phase in low-temperature-stable microemulsions. Langmuir 27:279–371
13. Hunger J, Stoppa A, Buchner R, Hefter G (2009) Dipole correlations in the ionic liquid 1-N-ethyl-3-N-methylimidazolium ethylsulfate and its binary mixtures with dichloromethane. J Phys Chem 113:9527–9537
14. Fernández A, Torrecilla JS, García J, Rodríguez F (2007) Thermophysical properties of 1-ethyl-3-methylimidazolium ethylsulfate and 1-butyl-3-methylimidazolium methylsulfate ionic liquids. J Chem Eng Data 52:1979–1983
15. Kelkar MS, Shi W, Maginn EJ (2008) Transport properties of 1-ethyl-3-methylimidazolium ethylsulfate and its mixtures with water. Ind Eng Chem Res 47:9115–9126
16. Domańska U, Laskowska M (2008) Phase equilibria and volumetric properties of (1-ethyl-3-methylimidazolium ethylsulfate + alcohol or water) binary systems. J Solut Chem 37:1271–1287
17. Arce A, Pobudkowska A, Rodríguez O, Soto A (2007) Citrus essential oil terpenless by extraction using 1-ethyl-3-

methylimidazolium ethylsulfate ionic liquid: effect of the temperature. Chem Eng J 133:213–218
18. Arce A, Rodríguez O, Soto A (2006) A comparative study on solvents for separation of tert-amyl ethyl ether and ethanol mixtures. New experimental data for 1-ethyl-3-methyl imidazolium ethyl sulfate ionic liquid. Chem Eng Sci 61:6929–6935
19. Alonso L, Arce A, Francisco M, Soto A (2008) Thiophene separation from aliphatic hydrocarbons using the 1-ethyl-3-methylimidazolium ethylsulfate ionic liquid. Fluid Phase Equilibria 270:97–102
20. Shi QF, Zhang Y, Jing GL, Kan JQ (2007) Properties of polyaniline synthesized in ionic liquid (l-ethyl-methylimidazolium-ethyl sulphate). Iran Polym J 16:337–344
21. Taghvaei V, Habibi-Yangjeh A, Behboudnia M (2009) Preparation and characterization of SnO_2 nanoparticles in aqueous solution of [EMIM][$EtSO_4$] as a low cost ionic liquid using ultrasonic irradiation. Powder Technol 195:63–67
22. Santafe AAM, Doumeche B, Blum LJ, Girard-Egrot AP, Marquette CA (2010) 1-ethyl-3-methylimidazolium ethylsulfate/copper catalyst for the enhancement of glucose chemiluminescent detection: effects on light emission and enzyme activity. Anal Chem 82:2401–2404
23. Jalili AH, Mehdizadeh A, Shokouhi M, Ahmadi AN, Hosseini-Jenab M, Fateminassab F (2010) Solubility and diffusion of CO_2 and H_2S in the ionic liquid 1-ethyl-3-methylimidazolium ethylsulfate. J Chem Thermodyn 42:1298–1303
24. Jiang Y, Wang A, Kan JQ (2007) Selective uricase biosensor based on polyaniline synthesized in ionic liquid. Sens Actuators B 124:529–534
25. Tan YY, Guo XX, Zhang JH, Kan JQ (2010) Amperometric catechol biosensor based on polyaniline-polyphenol oxidase. Biosens Bioelectron 25:1681–1687
26. Wang P, Liu M, Kan JQ (2009) Amperometric phenol biosensor based on polyaniline. Sens Actuators B 140:577–584
27. Ndiaye C, Xu SY, Wang Z (2009) Steamblanchingeffect on polyphenoloxidase, peroxidase and colour of mango (Mangifera indica L.) slices. Food Chem 113:92–95
28. Shi QF, Wang P, Jiang YL, Kan JQ (2008) Glucose biosensor based on polyaniline synthesized in ionic liquid. Biocatal Biotransform 27:54–59
29. Li S, Tan Y, Wang P, Kan JQ (2010) Inhibition of benzoic acid on the polyaniline-polyphenol oxidase biosensor. Sens Actuators B 144:18–22
30. Bernardes CES, Minas da Piedade ME, Canongia Lopes JN (2011) The structure of aqueous solutions of a hydrophilic ionic liquid: the full concentration range of 1-ethyl-3-methylimidazolium ethylsulfate and water. J Phys Chem B 115:2101–2116
31. Li L, Huang Y, Yan G, Liu F, Huang Z, Ma Z (2009) Poly (3, 4-ethylenedioxythiophene) nanospheres synthesized in magnetic ionic liquid. Mater Lett 63:8–10
32. Damlin P, Kvarnstrom C, Ivaska A (2004) Electrochemical synthesis and in situ spectroelectrochemical characterization of poly (3, 4-ethylenedioxythiophene) in room temperature ionic liquids. J Electroanal Chem 570:113–122
33. Dobbelin M, Marcilla R, Pozo-Gonzalo C, Mecerreyes D (2010) Innovative materials and applications based on poly (3, 4-ethylenedioxythiophene) and ionic liquids. J Mater Chem 20:7613–7622
34. Randriamahazaka H, Plesse C, Teyssié D, Chevrot C (2005) Relaxation kinetics of poly(3,4-ethylenedioxythiophene) in 1-ethyl-3-methylimidazolium bis ((trifluoromethyl) sulfonyl) amide ionic liquid during potential step experiments. Electrochim Acta 504:222–4229
35. Randriamahazaka H, Plesse C, Teyssié D, Chevrot C (2003) Electrochemical behaviour of poly(3,4-ethylenedioxythiophene) in a room-temperature ionic liquid. Electrochem Commun 5:613–617
36. Wagner K, Pringle JM, Hall SB, Forsyth M, MacFarlane DR, Officer DL (2005) Investigation of the electropolymerisation of EDOT in ionic liquids. Synth Met 153:257–260
37. Ahmad S, Deepa M, Singh S (2007) Electrochemical synthesis and surface characterization of poly (3, 4-ethylenedioxythiophene) films grown in an ionic liquid. Langmuir 23:11430–11433
38. Santhosh P, Manesh KM, Uthayakumar S, Komathi S, Gopalan AI, Lee KP (2009) Fabrication of enzymatic glucose biosensor based on palladium nanoparticles dispersed onto poly (3,4-ethylenedioxythiophene) nanofibers. Bioelectrochemistry 75:61–66
39. Merafín V, Agüí L, Yáñez-Sedeño P, Pingarrón J (2010) A novel hybrid platform for the preparation of disposable enzyme biosensors based on poly(3,4-ethylenedioxythiophene) electrodeposition in an ionic liquid medium onto gold nanoparticles-modified screen-printed electrodes. J Electroanal Chem 656:152–158
40. Aydogmus Z, Cetin SM, Ozgur MU (2002) Determination of ascorbic acid in vegetables by derivative spectrophotometry. Turk J Chem 26:697–704
41. Arya SP, Mahajan M, Jain P (1998) Photometric methods for the determination of vitamin C. Anal Sci 14:889–895
42. Arya SP, Mahajan M, Jain P (2000) Non-spectrophotometric methods for the determination of vitamin C. Anal Chim Acta 417:1–14
43. Ronkainen NJ, Halsall HB, Heineman WR (2010) Electrochemical biosensors. Chem Soc Rev 39:1747–1763
44. Rahman MA, Kumar P, Park DS, Shim YB (2008) Electrochemical sensors based on organic conjugated polymers. Sensors 8:118–141
45. Malinauskas A, Garjonyte R, Mazeikiene R, Jureviciute I (2004) Electrochemical response of ascorbic acid at conducting and electrogenerated polymer modified electrodes for electroanalytical applications: a review. Talanta 64:121–129
46. Dong B, Zhang SH, Zheng LQ, Xu JK (2008) Ionic liquid microemulsions: a new medium for electropolymerization. J Electroanal Chem 619–620:193–196
47. Liu M, Wen YP, Li D, Yue RR, Xu JK, He HH (2011) A stable sandwich-type amperometric biosensor based on poly(3,4-ethylenedioxythiophene)-single walled carbon nanotubes/ascorbate oxidase/nafion films for detection of L-ascorbic acid. Sens Actuators B 159:277–285
48. Liu M, Wen YP, Xu JK, He HH, Li D, Yue RR, Liu GD (2011) An amperometric biosensor based on ascorbate oxidase immobilized in poly(3,4-ethylenedioxythiophene)/multi-walled carbon nanotubes composite films for the determination of L-ascorbic acid. Anal Sci 27:477–482
49. Randriamahazaka H, Noel V, Chevrot C (1999) Nucleation and growth of poly (3, 4-ethylenedioxythiophene) in acetonitrile on platinum under potentiostatic conditions. J Electroanal Chem 472:103–111
50. Venables JA, Spiller GDT, Hanbucken M (1984) Nucleation and growth of thin film. Rep Prog Phys 47:399–459
51. Wen YP, Xu JK, He HH, Lu BY, Li YZ, Dong B (2009) Electrochemical polymerization of 3,4-ethylenedioxythiophene in aqueous micellar solution containing biocompatible amino acid-based surfactant. J Electroanal Chem 634:49–58
52. Peng C, Jin J, Chen GZ (2007) A comparative study on electrochemical co-deposition and capacitance of composite films of conducting polymers and carbon nanotubes. Electrochim Acta 53:525–537
53. Zhang GQ, Zhao YQ, Tao F, Li HL (2006) Electrochemical characteristics and impedance spectroscopy studies of nano-cobalt silicate hydroxide for supercapacitor. J Power Sources 161:723–729
54. Bobacka J, Lewenstam A, Ivaska A (2000) Electrochemical impedance spectroscopy of oxidized poly (3, 4-ethylenedioxythiophene) film electrodes in aqueous solutions. J Electroanal Chem 489:17–27
55. Li G, Pickup PG (2000) Ion transport in poly (3, 4-ethylenedioxythiophene)-poly (styrene-4-sulfonate) composites. Phys Chem Chem Phys 2:1255–1260